

This document is confidential and is proprietary to the American Chemical Society and its authors. Do not copy or disclose without written permission. If you have received this item in error, notify the sender and delete all copies.

Nanoantenna-enhanced light-matter interaction in atomically thin WS₂

Journal:	<i>ACS Photonics</i>
Manuscript ID:	ph-2015-00123x.R2
Manuscript Type:	Article
Date Submitted by the Author:	24-Jul-2015
Complete List of Authors:	Kern, Johannes; University of Münster, Trügler, Andreas; Institute of Physics, Karl-Franzens-University Graz, Theoretical Physics Niehues, Iris; University of Münster, Ewering, Johannes; University of Münster, Schmidt, Robert; University of Münster, Schneider, Robert; University of Münster, Najmaei, Sina; Rice University, George, Antony; Rice University, Department of Mechanical Engineering and Materials Science Zhang, Jing; Rice University, Materials Science and NanoEngineering Lou, Jun; Rice University, Materials Science and NanoEngineering Hohenester, Ulrich; Karl-Franzens-University Graz, Physics Michaelis, Steffen; University of Münster, Bratschitsch, Rudolf; Universität Münster, Physikalisches Institut

SCHOLARONE™
Manuscripts

Nanoantenna-enhanced light-matter interaction in atomically thin WS₂

Johannes Kern[†], Andreas Trügler[‡], Iris Niehues[†], Johannes Ewering[†], Robert Schmidt[†], Robert Schneider[†], Sina Najmaei[§], Antony George[§], Jing Zhang[§], Jun Lou[§], Ulrich Hohenester[‡], Steffen Michaelis de Vasconcellos[†] & Rudolf Bratschitsch^{†*}

[†]Institute of Physics and Center for Nanotechnology, University of Münster, 48149 Münster, Germany

[‡]Institute of Physics, University of Graz, 8010 Graz, Austria

[§]Department of Mechanical Engineering and Material Science, Rice University, Houston, Texas 77005, USA

KEYWORDS: Plasmonics, nanoantenna, 2D materials, transition metal dichalcogenides, WS₂, photoluminescence, dark-field scattering.

ABSTRACT: Atomically thin transition metal dichalcogenides (TMDCs) are an emerging class of two-dimensional semiconductors. Recently, first opto-electronic devices featuring photodetection as well as electroluminescence have been demonstrated using monolayer TMDCs as active material. However, the light-matter coupling for atomically thin TMDCs is limited by their small absorption length and low photoluminescence quantum yield. Here, we significantly increase the light-matter interaction in monolayer tungsten disulphide (WS₂) by coupling the atomically thin semiconductor to a plasmonic nanoantenna. Due to the plasmon resonance of the nanoantenna, strongly enhanced optical near-fields are generated within the WS₂ monolayer. We observe an increase in

1
2
3 **photoluminescence intensity by more than one order of magnitude, resulting from a**
4 **combined absorption and emission enhancement of the exciton in the WS₂ monolayer. The**
5 **polarization characteristics of the coupled system are governed by the nanoantenna. The**
6 **robust nanoantenna-monolayer hybrid paves the way for efficient photodetectors, solar**
7 **cells, and light emitting devices based on two-dimensional materials.**
8
9

10
11
12
13
14
15
16
17 Tailoring the interaction between light and matter is crucial for the performance of optical and
18 opto-electronic devices. Solar cells, photodetectors, and optical transistors rely on their ability to
19 efficiently absorb light. Light emitting devices benefit from a high radiative efficiency of the
20 active material. One strategy to improve device performance is to identify novel materials, which
21 exhibit an intrinsically strong light-matter interaction. Recently, an extraordinary optical
22 response of atomically thin transition metal dichalcogenides (TMDCs) has been reported¹.
23 Monolayers of MoS₂, MoSe₂, WS₂, and WSe₂ exhibit an optical band gap²⁻⁵ and are therefore
24 interesting for opto-electronic devices such as photodetectors and light emitting devices⁶⁻¹¹.
25 However, the absorption is limited by the atomic thickness of the TMDC monolayers.
26 Concerning light emission, atomically thin TMDCs exhibit a direct optical band gap with a
27 photoluminescence yield, which is orders of magnitude larger than for bulk crystals². However,
28 in absolute numbers the observed photoluminescence quantum yield of 10⁻³ is low².
29 Consequently, for practical device applications, strategies for increasing the light-matter
30 interaction are needed.
31
32
33
34
35
36
37
38
39
40
41
42
43
44
45
46
47
48
49

50 Plasmonic nanoantennas made of noble metals enhance the light-matter interaction and control
51 light on the nanoscale¹²⁻¹⁴. Excitation of the antenna resonance leads to intense optical fields in
52 the vicinity of the antenna. In this region of high photonic density of states the absorption as well
53
54
55
56
57
58
59
60

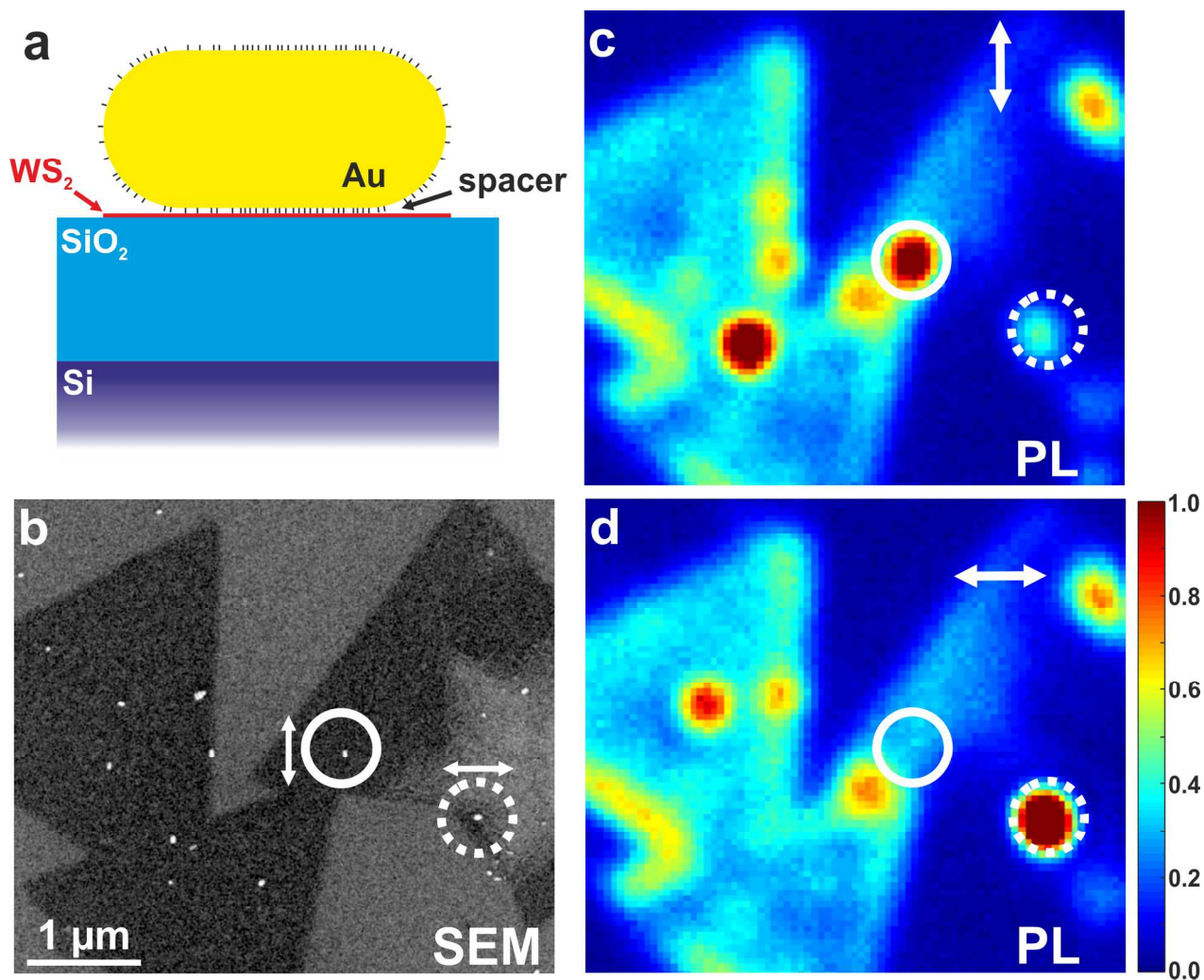
1
2
3 as the emission of photons can be significantly enhanced. By coupling to a plasmonic antenna
4
5 strong enhancement of the fluorescence^{15,16} and Raman¹⁷ response of single molecules has been
6
7
8 achieved. The efficiency of photodetectors and solar cells based on bulk semiconductors^{18,19} has
9
10 been improved.

11
12
13 Recently, plasmonic nanostructures have been placed above and below MoS₂ monolayers²⁰⁻²⁵.
14
15
16 Interesting phenomena such as a reversible structural phase transition in MoS₂ due to hot
17
18 electron injection²³ or a thermally-induced spectral modification of photoluminescence²⁴ have
19
20 been observed. However, so far little attention has been paid to the design of the plasmonic
21
22 nanostructures. As a consequence, the reported photoluminescence enhancements were only two-
23
24 fold at best^{22,24}. Even photoluminescence quenching was observed²¹. Photoluminescence
25
26 enhancement was attributed to an increased absorption. Here, we demonstrate an enhancement in
27
28 both absorption and emission, leading to a record photoluminescence increase by one order of
29
30 magnitude from an atomically thin semiconductor. We use a novel hybrid system consisting of a
31
32 WS₂ monolayer and a single-crystalline plasmonic nanoantenna. In a combined numerical and
33
34 experimental study we demonstrate that in this way a hybrid plasmon-exciton system is formed.
35
36
37 The hybrid nature is revealed by the observation of a six-fold (four-fold) PL intensity
38
39 enhancement with respect to a WS₂ monolayer without antenna when excitation (emission)
40
41 polarization is matched to the antenna. Our analysis on single nanoantennas unambiguously
42
43 shows that the coupling results from the enhanced plasmonic near-fields at the position of WS₂
44
45 monolayer. We are also able to control the shape of the photoluminescence spectrum with the
46
47 help of the antenna by tuning the plasmonic resonance via the antenna length. Our work provides
48
49 important groundwork for the design of future nanoantenna-enhanced photodetectors, solar cells,
50
51 and light emitting devices based on two-dimensional materials.
52
53
54
55
56
57
58
59
60

1
2
3 Figure 1a shows a schematic drawing of the investigated hybrid system of plasmonic
4 nanoantenna and atomically thin WS₂ layer. The WS₂ monolayers are grown on SiO₂/Si substrate
5 by chemical vapor deposition (CVD)²⁶ using WO₃ powder as a precursor and an evaporation
6 temperature close to 800°C. The antennas are single-crystalline, chemically-grown gold
7 nanorods with a diameter of 30 nm and lengths ranging from 55 to 70 nm. The rods are obtained
8 in aqueous solution from Nanopartz Inc. and diluted to a concentration of 10¹⁰ particles/mL. 1
9 μL of the solution is drop-cast onto monolayers of tungsten disulphide (WS₂) on SiO₂/Si
10 substrate. The gold nanorods are functionalized by a molecular layer (Cetyl-Trimethyl-
11 Ammoniumbromid, CTAB), which acts as a spacer between gold and WS₂. In the electron
12 micrograph of Fig. 1 atomically thin WS₂ monolayers of triangular shape appear dark. Gold
13 nanorods on top of the monolayer are bright and can be clearly identified. Due to the drop-
14 casting process, the gold nanorods are randomly oriented on the WS₂ monolayers. In Fig. 1b a
15 horizontally aligned rod is marked by a dashed white circle and a rod with vertical orientation by
16 a solid circle (see Fig. S1 for images at high magnification).
17
18
19
20
21
22
23
24
25
26
27
28
29
30
31
32
33
34
35
36

37 Photoluminescence intensity maps recorded for excitation with circularly polarized light at a
38 wavelength of $\lambda_{\text{ex}} = 588$ nm and selection of vertical and horizontal emission polarization are
39 presented in Fig. 1c and d, respectively. Photoluminescence emission is collected with an
40 objective lens with a numerical aperture NA = 0.9 and detected via a spectrometer (Andor,
41 Shamrock SR-303i) equipped with a cooled sCMOS camera (Andor, DC-152-Q-C00_DI). The
42 photoluminescence emission from the WS₂ monolayer alone shows no polarization dependence
43 and is homogenous across the flake. However, stronger luminescence is typically observed at the
44 edge of the WS₂ flakes²⁷. At position of the gold nanoantennas the photoluminescence is strongly
45 enhanced by a factor of 4.5 for the horizontally aligned rod and 2.5 for the vertically aligned rod.
46
47
48
49
50
51
52
53
54
55
56
57
58
59
60

1
2
3 If both excitation and emission polarization are matched to the antenna we observe an
4 enhancement of up to 11 (Fig. S2 and discussion below). For the hybrid antenna-monolayer
5 system the photoluminescence is polarization dependent and is strongest for polarization along
6 the long nanoantenna axis. If the polarization is perpendicular to the nanorod, the luminescence
7 intensity is significantly lower and is similar to locations on the WS₂ monolayer without gold
8 nanorods. We also observe intrinsic gold nanorod photoluminescence²⁸. However, it is
9 comparatively very weak, as evident from nanorods at sample positions without WS₂ (top left
10 corner of Fig. 1b - d).
11
12
13
14
15
16
17
18
19
20
21
22
23



1
2
3 **Figure 1.** (a) Schematic drawing of the sample. (b) Electron micrograph of monolayer WS₂ (dark
4 triangles) with gold nanorods on top (bright rods). Solid (dashed) circles mark a rod with vertical
5 and (horizontal) orientation. (c, d) Normalized photoluminescence intensity map of the region
6 shown in (b). White arrows indicate the emission polarization. Strongest PL enhancement is
7 found for orientation of the nanoantenna along the polarization direction.
8
9

10
11
12
13
14
15
16 In order to understand the strong PL enhancement and elucidate the nature of the coupling
17 between the nanoantenna and the atomically thin semiconductor, we have to determine the
18 spectral position of the plasmon and exciton resonances. The strength of the light-matter
19 interaction of the hybrid system strongly depends on their spectral overlap. We first investigate
20 the resonances of the constituents of the hybrid system - the nanoantenna and the WS₂
21 monolayer.
22
23
24
25
26
27
28
29

30
31 Single-crystalline gold nanorods are efficient optical antennas and exhibit intense optical near-
32 fields and enhanced scattering at their longitudinal plasmon resonance¹³. The position of the
33 plasmon resonance can be tuned by the length of the nanoantenna¹³. The dark field scattering
34 spectrum of a single 65 nm long antenna clearly shows a pronounced longitudinal plasmon
35 resonance at 607 nm, as well as the weak transverse plasmon resonance at 526 nm (Fig. 2a).
36
37
38
39
40
41
42
43

44 The spectral positions of the excitonic resonances of the atomically thin semiconductor are also
45 obtained from dark field scattering spectra from the edges of WS₂ monolayers (Fig. 2b). The
46 spectra show two distinct maxima at the A and B exciton wavelengths of 618 nm and 565 nm.
47
48
49 The peak positions vary from flake to flake and are in good agreement with absorption spectra
50 (see supplementary material Fig. S3).
51
52
53
54
55
56
57
58
59
60

1
2
3 Our investigated hybrid system consists of monolayer WS₂ and a gold nanorod of three different
4 lengths (55, 60, and 70 nm) and a diameter of 25 nm. The dimensions of the antenna are chosen
5 such that the longitudinal plasmon resonance of the nanoantenna can be tuned across the A
6 exciton resonance of the monolayer. The B exciton is always off-resonant to the longitudinal
7 nanoantenna resonance and shows no polarization-dependence of the photoluminescence, similar
8 to the A exciton of the WS₂ monolayer without antenna. In the measured dark field scattering
9 spectra (Fig. 2c-e) a clear shift of the longitudinal plasmon resonance from 600 to 650 nm is
10 observed, if the antenna length is increased from 55 to 70 nm and the emission polarization is
11 selected along the long antenna axis. We find a prominent narrow minimum in the broad
12 plasmon resonance in the scattering spectra of the hybrid system with the two short antennas
13 (Fig. 2c, d). The spectral position of the dip is independent of the antenna length and occurs at
14 the wavelength of the A exciton. For the longest antenna (70 nm) there is only small spectral
15 overlap between plasmon and exciton. Consequently, the coupling is weak and the minimum in
16 the plasmon resonance disappears.

17
18
19
20
21
22
23
24
25
26
27
28
29
30
31
32
33
34
35
36
37 Our experimental results are in excellent agreement with numerically calculated scattering
38 spectra (Fig. 2g-i). The simulations are performed with the MNPBEM toolbox^{29, 30}, which uses
39 the boundary element (BEM) approach³¹. We assume an antenna diameter of 30 nm and take a
40 distance of 0.5 nm between antenna and WS₂ into account (see supplementary Fig. S4 for the
41 distance dependence). In Fig. 2f the calculated electric field distribution for the hybrid system is
42 shown with polarization along the long antenna axis at the wavelength of the A exciton. Intensity
43 enhancements as high as 6 are obtained at position of the WS₂ monolayer. For polarization
44 perpendicular to the antenna axis no enhancement is found with respect to the WS₂ monolayer
45
46
47
48
49
50
51
52
53
54
55
56
57
58
59
60

without antenna and only a weak scattering signal is observed in the experiment (blue curves in Fig. 2c-e).

In summary, we find that the A exciton of the atomically thin WS_2 monolayer couples to the metal nanoantenna via the enhanced plasmonic near-field, which leads to a pronounced minimum in the scattering spectra. The strength of this dip critically depends on polarization as well as spectral position of the plasmon with respect to the A exciton.

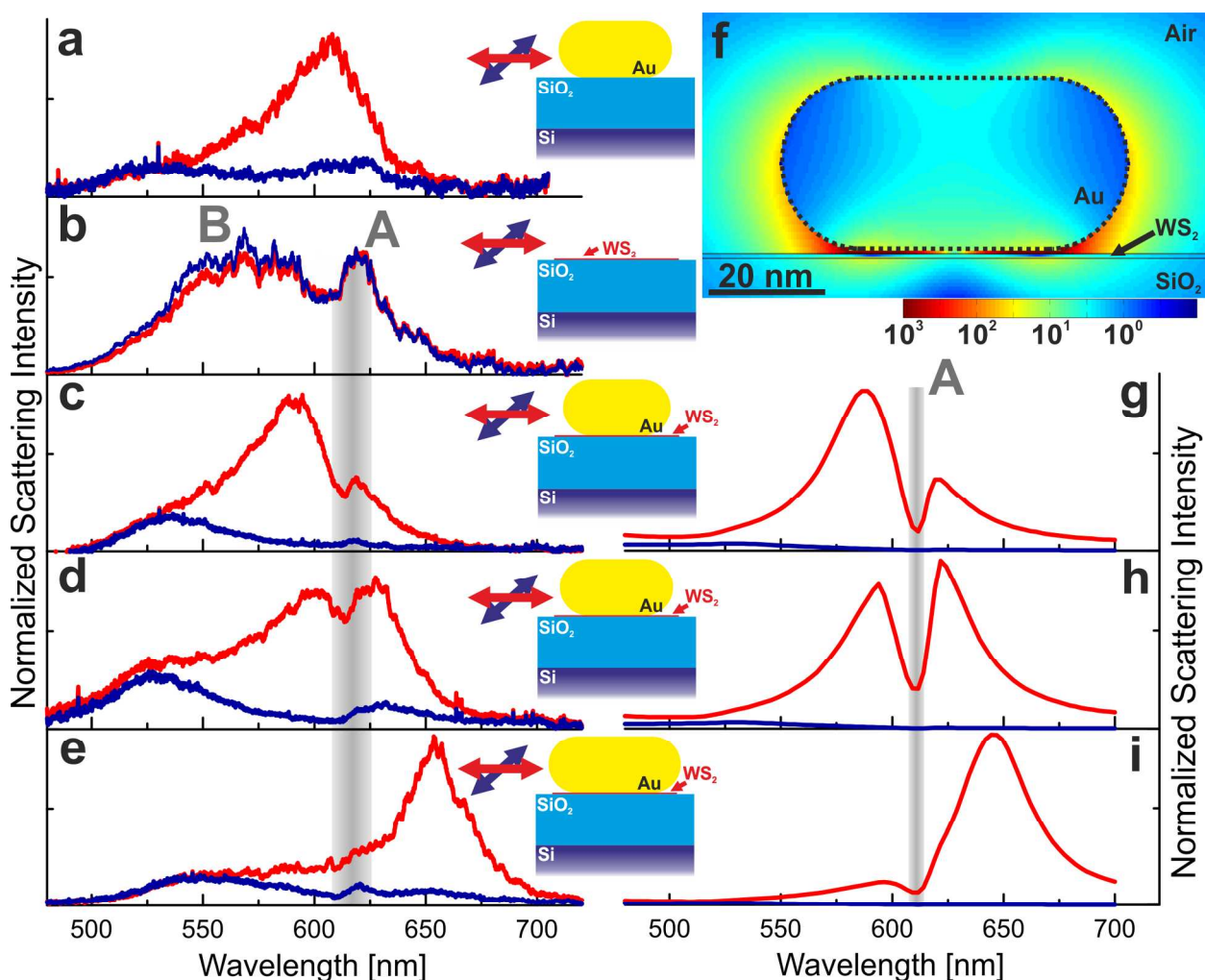


Figure 2. (a) Polarization resolved scattering spectrum of a 65 nm long gold nanorod on SiO_2/Si

1
2
3 substrate. (b) Scattering spectrum of a monolayer WS₂ flake on SiO₂/Si substrate. (c-e)
4
5 Measured emission-polarization resolved scattering spectra of nanorods coupled to monolayer
6
7 WS₂ on SiO₂/Si substrate. The length of the nanorods is 55, 60 and 70 nm in (c, d, e),
8
9 respectively. Polarization directions along/across the nanoantenna axis are indicated by coloured
10
11 arrows. The vertical line marks the position of the A exciton of monolayer WS₂ at 618±10 nm.
12
13 (f) Calculated near-field intensity map on a logarithmic scale at 612 nm wavelength (A exciton)
14
15 and polarization along the nanorod axis. (g-i) Calculated emission-polarization resolved
16
17 scattering spectra of nanorods coupled to monolayer WS₂ on SiO₂/Si substrate. The length of the
18
19 nanorods is 60, 65 and 75 nm in (g, h, i), respectively.
20
21
22
23
24

25 Having elucidated the different resonances and coupling of the hybrid system, we return to the
26
27 prominent photoluminescence enhancement of Fig. 1c, d. In particular, we quantify how the
28
29 electric field enhancement results in an absorption and emission enhancement of the hybrid
30
31 system (Fig. 3). A hybrid system with a central wavelength of the plasmon resonance at 625 nm
32
33 is chosen for this investigation, because the broad plasmon resonance overlaps well with the
34
35 excitation wavelength of 588 nm as well as with the exciton emission at 618 nm.
36
37
38
39

40 First, we study a WS₂ monolayer without nanoantenna (see supplementary Fig. S5 for a
41
42 photoluminescence spectrum). We find that the PL spectrum is dominated by the A exciton⁴. The
43
44 PL intensity does not depend on excitation or emission polarization. For excitation with 532 nm
45
46 light the PL intensity is a factor of two higher than for excitation with 588 nm. This effect is due
47
48 to the different absorption (factor of two) at the two excitation wavelengths.
49
50
51
52

53 The hybrid nanoantenna-monolayer system exhibits a strikingly different behavior, if excited at
54
55 the plasmon resonance with 588 nm light (Fig. 3a-d). For excitation (Fig. 3a, b) and emission
56
57
58
59
60

1
2
3 polarization (Fig. 3c, d) perpendicular to the nanoantenna axis the PL intensity is similar to the
4
5 WS₂ monolayer without nanoantenna. However, the photoluminescence strongly increases, if the
6
7 excitation as well as emission polarization is chosen along the nanorod axis (Fig. 3a-d). This
8
9 enhancement arises from the strong optical near-fields created by the longitudinal plasmon
10
11 resonance of the nanoantenna, which penetrate the WS₂ monolayer and extend over a region of
12
13 80 x 30 nm² (Fig. 2f). Excitons located in the enhanced electric field region experience an
14
15 increased absorption as well as an increased emission rate. The latter effect results in a higher
16
17 emission quantum yield of the hybrid system. In our experiment the PL enhancement is clearly
18
19 observed by comparing the polarization-resolved PL of the hybrid nanoantenna-monolayer
20
21 system to the WS₂ monolayer alone (Fig. 3b for excitation and 3c for emission). Whereas the
22
23 photoluminescence of the WS₂ monolayer is unpolarized (circle), a clear dipolar-like pattern is
24
25 observed for excitation and emission polarization of the hybrid system. To study the emission
26
27 polarization, the system was excited by circularly polarized light. The PL signal of the hybrid
28
29 system is a factor of 6.4 (4.5) larger compared to the PL of the monolayer alone, when the
30
31 excitation (emission) polarization is matched to the antenna axis. These high values underline the
32
33 increased coupling of the nanoantenna with the atomically thin semiconductor. The fact that
34
35 absorption enhancement plays a more important role than emission enhancement is revealed by
36
37 investigating the identical hybrid system with off-resonant excitation at a wavelength of 532 nm.
38
39 In this case the PL intensity is more than ten times lower than for resonant excitation at 588 nm.
40
41 If the excitation polarization is perpendicular to the long antenna axis, the PL intensity resembles
42
43 that of a WS₂ monolayer without nanoantenna. For excitation polarization along the antenna axis
44
45 the PL is increased by a factor of 1.3 (Fig. 3e, f). Even though the excitation is off-resonant, the
46
47
48
49
50
51
52
53
54
55
56
57
58
59
60

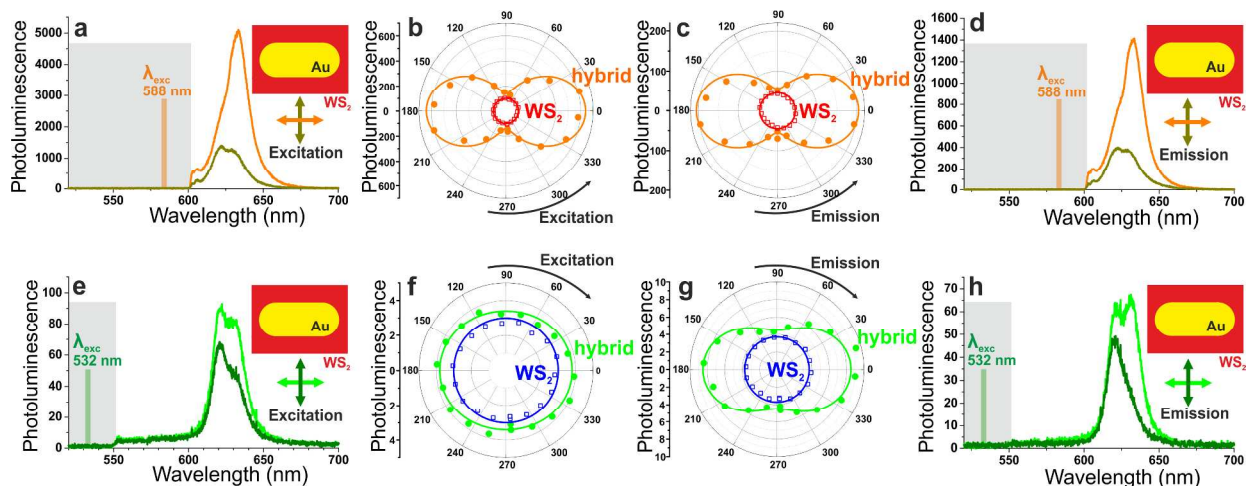


Figure 3. (a-d) PL spectrum and angular dependence for an excitation wavelength of 588 nm. (e-h) PL spectrum and angular dependence for excitation wavelength of 532 nm. (a, e) PL spectrum with excitation polarization along and across the antenna. (b, f) PL intensity of a WS_2 monolayer without nanoantenna and the nanoantenna-monolayer hybrid depending on the excitation polarization. (c, g) PL intensity of a WS_2 monolayer without nanoantenna and the nanoantenna-monolayer hybrid depending on the emission polarization. (d, h) PL spectrum with emission polarization along and across the antenna axis for circularly polarized excitation. Grey shaded regions in the spectra indicate band pass filters to block light from the laser used for excitation. Solid lines drawn in the angular plots model the polarization dependence by a sum of a single horizontally orientated dipole (two-lobed) and randomly oriented dipoles (circle).

plasmon and exciton resonances still overlap, and the emission rate is expected to increase. Indeed, the PL signal is 2.3 times stronger for emission polarization along the antenna axis (Fig. 3g, h).

Considering the fact that the spatial extension of the enhanced optical near-fields of the nanoantenna penetrating the WS_2 monolayer is a factor of 100 smaller than the diffraction-

1
2
3 limited collection area of PL light, the local PL enhancement is estimated to be 1000. Moreover,
4
5 it should be noted that even the highest applied continuous wave excitation power density of 14
6
7 kW/cm² is well below saturation of this hybrid system (supplementary Fig. S6). Much stronger
8
9 enhancement can be expected for even higher excitation powers, where the saturation of the WS₂
10
11 monolayer can be compensated by an increased emission rate.
12
13
14
15

16 It is expected that an increased emission rate due to the antenna resonance not only enhances the
17
18 PL intensity but also modifies the PL spectrum³². To this end we record emission-polarization
19
20 resolved photoluminescence spectra for excitation with circular polarization with an excitation
21
22 wavelength of 588 nm (Fig. 4). We investigate three antenna-WS₂ hybrids with previously
23
24 characterized plasmon resonance (Fig. 2 c-e). For emission polarization set perpendicular to the
25
26 nanoantenna axis the photoluminescence spectrum resembles that of a WS₂ monolayer.
27
28 However, for emission polarization along the antenna axis the spectrum is enhanced at the
29
30 plasmon resonance. The modification strongly depends on the length of the antenna, which
31
32 further demonstrates the coupling of exciton and plasmon. The fact that spectral modification of
33
34 the PL is only observed for emission polarization along the antenna suggests that it originates
35
36 from an enhanced emission rate and we can exclude thermal effects²⁴ as well as morphology
37
38 changes²³ of the WS₂ monolayers.
39
40
41
42
43
44

45 It should be noted that we have observed robust photoluminescence of the hybrid nanoantenna-
46
47 monolayer systems over a time period of several months, which allowed us to conduct
48
49 systematic studies on a single nanostructure. This behavior is in stark contrast to earlier
50
51 experiments of antenna-enhanced fluorescence of single molecules, where enhanced
52
53 fluorescence was only observed for a few 100 ms before photobleaching occurred¹⁶.
54
55
56
57
58
59
60

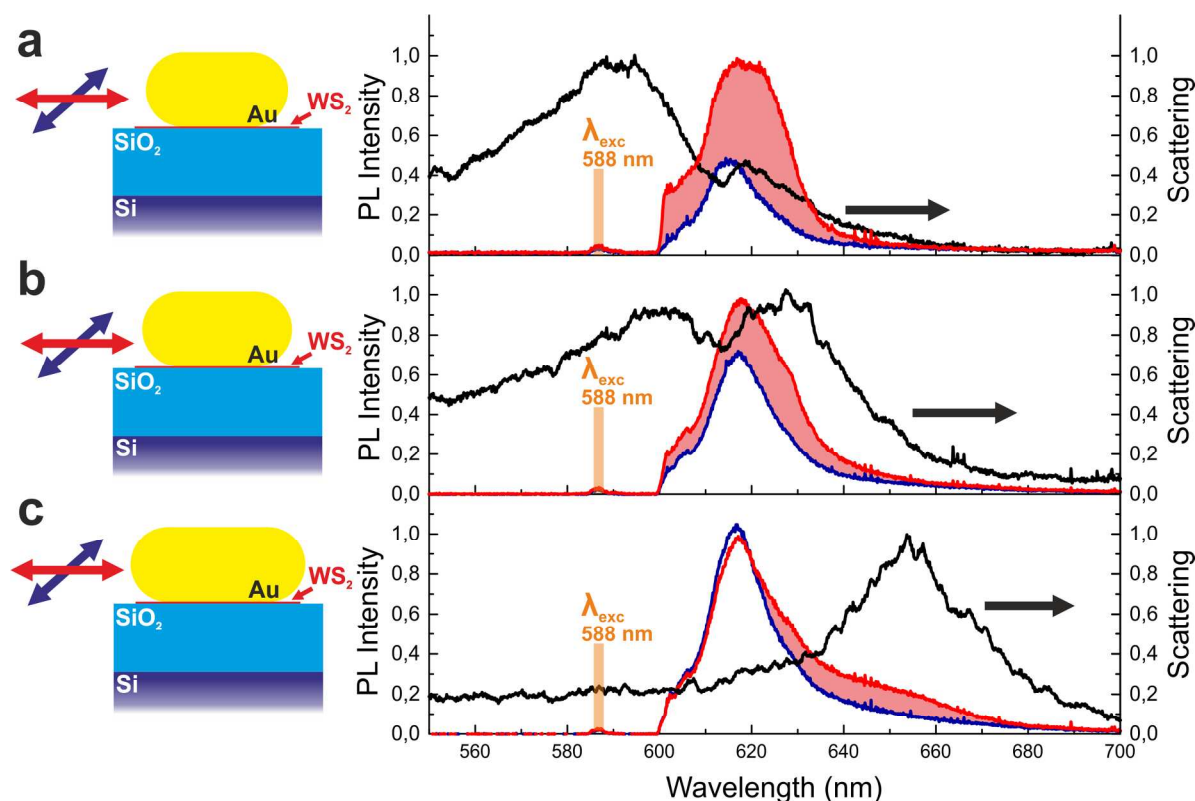


Figure 4. (a-c) Emission-polarization resolved photoluminescence spectra (colored lines) of an antenna-WS₂ hybrid compared to scattering spectra (black lines). PL spectra are excited with circular polarization with an excitation wavelength of 588 nm. The direction of emission polarization along/across the nanoantenna long axis is indicated by arrows. The investigated antennas are the same as in Fig. 2 c-e, with nanorod lengths of 55, 60 and 70 nm in (a, b, c), respectively.

In conclusion, we have demonstrated antenna-enhanced light-matter coupling in atomically thin WS₂. Due to intense optical near-fields provided by the metal nanoantenna we observe an absorption as well as emission enhancement, resulting in a one order of magnitude increase of the photoluminescence of the WS₂ monolayer. We find that the polarization characteristics as

1
2
3 well as the photoluminescence spectrum are modified by the longitudinal plasmon resonance.
4
5 The robust hybrid nanoantenna-monolayer system lights the way to efficient photodetectors,
6
7 solar cells, light emitting and conceptually new valleytronic devices based on two-dimensional
8
9 materials.
10
11

12
13
14 Note added: During the review process we became aware of a related study³³ of Ag nanodisc
15
16 arrays fabricated by electron-beam lithography on monolayer MoS₂.
17
18

19 ASSOCIATED CONTENT

20
21
22
23 **Supporting Information.** Photoluminescence enhancement of monolayer WS₂ with both
24
25 excitation and emission polarization matched to the nanoantenna; Absorption spectrum of a WS₂
26
27 monolayer; Numerically calculated scattering spectra of the antenna-WS₂ hybrid as a function of
28
29 the distance between antenna and WS₂; Photoluminescence of the WS₂ monolayer without
30
31 nanoantenna; Photoluminescence intensity depending on excitation power; Details of the
32
33 simulation technique. This material is available free of charge via the Internet at
34
35 <http://pubs.acs.org>.
36
37
38

39 AUTHOR INFORMATION

40 41 42 43 **Corresponding Author**

44
45
46 *Rudolf.Bratschitsch@uni-muenster.de
47
48

49 **Notes**

50
51
52 The authors declare no competing financial interest.
53
54

55 ACKNOWLEDGMENT

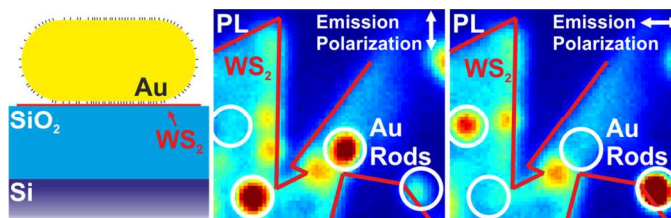
We gratefully acknowledge financial support by the Deutsche Forschungsgemeinschaft (SPP 1391).

REFERENCES

1. Wang, Q. H.; Kalantar-Zadeh, K.; Kis, A.; Coleman, J. N.; Strano, M. S. Electronics and Optoelectronics of Two-Dimensional Transition Metal Dichalcogenides. *Nat. Nanotechnol.* **2012**, *7*, 699–712.
2. Mak, K. F.; Lee, C.; Hone, J.; Shan, J.; Heinz, T. F. Atomically Thin MoS₂: A New Direct-Gap Semiconductor. *Phys. Rev. Lett.* **2010**, *105*, 136805.
3. Splendiani, A.; Sun, L.; Zhang, Y.; Li, T.; Kim, J.; Chim, C.-Y.; Galli, G.; Wang, F. Emerging Photoluminescence in Monolayer MoS₂. *Nano Lett.* **2010**, *10*, 1271–1275.
4. Zhao, W.; Ghorannevis, Z.; Chu, L.; Toh, M.; Kloc, C.; Tan, P.-H.; Eda, G. Evolution of Electronic Structure in Atomically Thin Sheets of WS₂ and WSe₂. *ACS Nano* **2013**, *7*, 791–797.
5. Tonndorf, P.; Schmidt, R.; Böttger, P.; Zhang, X.; Börner, J.; Liebig, A.; Albrecht, M.; Kloc, C.; Gordan, O.; Zahn, D. R.; et al. Photoluminescence Emission and Raman Response of Monolayer MoS₂, MoSe₂, and WSe₂. *Opt. Express* **2013**, *21*, 4908–4916.
6. Lopez-Sanchez, O.; Lembke, D.; Kayci, M.; Radenovic, A.; Kis, A. Ultrasensitive Photodetectors Based on Monolayer MoS₂. *Nat. Nanotechnol.* **2013**, *8*, 497–501.
7. Yin, Z.; Li, H.; Li, H.; Jiang, L.; Shi, Y.; Sun, Y.; Lu, G.; Zhang, Q.; Chen, X.; Zhang, H. Single-Layer MoS₂ Phototransistors. *ACS Nano* **2012**, *6*, 74–80.
8. Pospischil, A.; Furchi, M. M.; Mueller, T. Solar-Energy Conversion and Light Emission in an Atomic Monolayer P-N Diode. *Nat. Nanotechnol.* **2014**, *9*, 257–261.
9. Baugher, B. W. H.; Churchill, H. O. H.; Yang, Y.; Jarillo-Herrero, P. Optoelectronic Devices Based on Electrically Tunable P-N Diodes in a Monolayer Dichalcogenide. *Nat. Nanotechnol.* **2014**, *9*, 262–267.
10. Ross, J. S.; Klement, P.; Jones, A. M.; Ghimire, N. J.; Yan, J.; Mandrus, D. G.; Taniguchi, T.; Watanabe, K.; Kitamura, K.; Yao, W.; et al. Electrically Tunable Excitonic Light-Emitting Diodes Based on Monolayer WSe₂ P-N Junctions. *Nat. Nanotechnol.* **2014**, *9*, 268–272.
11. Lee, C.-H.; Lee, G.-H.; van der Zande, A. M.; Chen, W.; Li, Y.; Han, M.; Cui, X.; Arefe, G.; Nuckolls, C.; Heinz, T. F.; et al. Atomically Thin P-n Junctions with van Der Waals Heterointerfaces. *Nat. Nanotechnol.* **2014**, *9*, 676–681.
12. Novotny, L.; van Hulst, N. Antennas for Light. *Nat. Photonics* **2011**, *5*, 83–90.
13. Biagioni, P.; Huang, J. S.; Hecht, B. Nanoantennas for Visible and Infrared Radiation. *Rep. Prog. Phys.* **2012**, *75*, 024402.
14. Merlein, J.; Kahl, M.; Zuschlag, A.; Sell, A.; Halm, A.; Boneberg, J.; Leiderer, P.; Leitenstorfer, A.; Bratschitsch, R. Nanomechanical Control of an Optical Antenna. *Nat. Photonics* **2008**, *2*, 230–233.
15. Kinkhabwala, A.; Yu, Z.; Fan, S.; Avlasevich, Y.; Müllen, K.; Moerner, W. E. Large Single-Molecule Fluorescence Enhancements Produced by a Bowtie Nanoantenna. *Nat. Photonics* **2009**, *3*, 654–657.
16. Khatua, S.; Paulo, P. M. R.; Yuan, H.; Gupta, A.; Zijlstra, P.; Orrit, M. Resonant Plasmonic Enhancement of Single-Molecule Fluorescence by Individual Gold Nanorods. *ACS Nano* **2014**, *8*, 4400–4449.
17. Nie, S. Probing Single Molecules and Single Nanoparticles by Surface-Enhanced Raman Scattering. *Science* **1997**, *275*, 1102–1106.
18. Knight, M. W.; Sobhani, H.; Nordlander, P.; Halas, N. J. Photodetection with Active Optical Antennas. *Science* **2011**, *332*, 702–704.
19. Atwater, H. A.; Polman, A. Plasmonics for Improved Photovoltaic Devices. *Nat. Mater.* **2010**, *9*, 205–213.
20. Lin, J.; Li, H.; Zhang, H.; Chen, W. Plasmonic Enhancement of Photocurrent in MoS₂ Field-Effect-Transistor. *Appl. Phys. Lett.* **2013**, *102*, 203109.
21. Bhanu, U.; Islam, M. R.; Tetard, L.; Khondaker, S. I. Photoluminescence Quenching in Gold - MoS₂ Hybrid Nanoflakes. *Sci. Rep.* **2014**, *4*.
22. Sobhani, A.; Lauchner, A.; Najmaei, S.; Ayala-Orozco, C.; Wen, F.; Lou, J.; Halas, N. J. Enhancing the Photocurrent and Photoluminescence of Single Crystal Monolayer MoS₂ with Resonant Plasmonic Nanoshells. *Appl. Phys. Lett.* **2014**, *104*, 031112.

- 1
2
3 23. Kang, Y.; Najmaei, S.; Liu, Z.; Bao, Y.; Wang, Y.; Zhu, X.; Halas, N. J.; Nordlander, P.; Ajayan, P. M.;
4 Lou, J.; et al. Plasmonic Hot Electron Induced Structural Phase Transition in a MoS₂ Monolayer. *Adv.*
5 *Mater.* **2014**, *26*, 6467–6471.
- 6 24. Najmaei, S.; Mlayah, A.; Arbouet, A.; Girard, C.; Léotin, J.; Lou, J. Plasmonic Pumping of Excitonic
7 Photoluminescence in Hybrid MoS₂–Au Nanostructures. *ACS Nano* **2014**, *8*, 12682–12689.
- 8 25. Goodfellow, K. M.; Beams, R.; Chakraborty, C.; Novotny, L.; Vamivakas, A. N. Integrated Nanophotonics
9 Based on Nanowire Plasmons and Atomically Thin Material. *Optica* **2014**, *1*, 149–152.
- 10 26. Najmaei, S.; Liu, Z.; Zhou, W.; Zou, X.; Shi, G.; Lei, S.; Yakobson, B. I.; Idrobo, J.-C.; Ajayan, P. M.; Lou,
11 J. Vapour Phase Growth and Grain Boundary Structure of Molybdenum Disulphide Atomic Layers. *Nat.*
12 *Mater.* **2013**, *12*, 754–759.
- 13 27. Gutiérrez, H. R.; Perea-López, N.; Elías, A. L.; Berkdemir, A.; Wang, B.; Lv, R.; López-Urías, F.; Crespi,
14 V. H.; Terrones, H.; Terrones, M. Extraordinary Room-Temperature Photoluminescence in Triangular WS₂
15 Monolayers. *Nano Lett.* **2013**, *13*, 3447–3454.
- 16 28. Tcherniak, A.; Dominguez-Medina, S.; Chang, W.-S.; Swanglap, P.; Slaughter, L. S.; Landes, C. F.; Link, S.
17 One-Photon Plasmon Luminescence and Its Application to Correlation Spectroscopy as a Probe for
18 Rotational and Translational Dynamics of Gold Nanorods. *J. Phys. Chem. C* **2011**, *115*, 15938–15949.
- 19 29. Hohenester, U.; Trügler, A. MNPBEM – A Matlab Toolbox for the Simulation of Plasmonic Nanoparticles.
20 *Comput. Phys. Commun.* **2012**, *183*, 370–381.
- 21 30. Waxenegger, J.; Trügler, A.; Hohenester, U. Plasmonics simulations with the MNPBEM toolbox:
22 Consideration of substrates and layer structures. *Comput. Phys. Commun.* **2015**, *138*, 193.
- 23 31. García de Abajo, F.; Howie, A. Retarded Field Calculation of Electron Energy Loss in Inhomogeneous
24 Dielectrics. *Phys. Rev. B* **2002**, *65*, 115418.
- 25 32. Ringler, M.; Schwemer, A.; Wunderlich, M.; Nichtl, A.; Kürzinger, K.; Klar, T.; Feldmann, J. Shaping
26 Emission Spectra of Fluorescent Molecules with Single Plasmonic Nanoresonators. *Phys. Rev. Lett.* **2008**,
27 *100*.
- 28 33. Butun, S.; Tongay, S.; Aydin, K. Enhanced Light Emission from Large-Area Monolayer MoS₂ Using
29 Plasmonic Nanodisc Arrays. *Nano Lett.* **2015**, *15* (4), 2700–2704.
- 30
31
32
33
34
35
36
37
38
39
40
41
42
43
44
45
46
47
48
49
50
51
52
53
54
55
56
57
58
59
60

1
2
3 For Table of Contents Use Only
4
5



Nanoantenna-enhanced light-matter interaction in atomically thin WS₂

Johannes Kern, Andreas Trügler, Iris Niehues, Johannes Ewering, Robert Schmidt, Robert Schneider, Sina Najmaei, Antony George, Jing Zhang, Jun Lou, Ulrich Hohenester, Steffen Michaelis de Vasconcellos & Rudolf Bratschitsch